Science
AAAS

Chlamydomonas Swims with Two "Gears" in a Eukaryotic Version of Run-and-Tumble Locomotion

Marco Polin, *et al.*

Science **325**, 487 (2009);
DOI: 10.1126/science.1172667

A strains of the H1N1 subtype replicate efficiently in mice only after they are adapted to growth in these animals (*21*). The MID_{50} titers, determined through the detection of virus in the lungs of mice 3 days after inoculation, were markedly low (MID_{50} = $10^{0.5–1.5}$ PFU or EID_{50}), indicating high infectivity in this model. We next determined whether 2009 A(H1N1) influenza viruses replicated systemically in the mouse after intranasal infection, a characteristic of virulent avian influenza (H5N1) viruses isolated from humans but not of 1918 (H1N1) virus (*17*, *22*). All mice infected with CA/04, TX/15, or MX/4108 viruses had undetectable levels (<10 PFU/ml) of virus in whole spleen, thymus, brain, and intestinal tissues, indicating that the 2009 A(H1N1) influenza viruses did not spread to extrapulmonary organs in the mouse.

The full clinical spectrum of disease caused by 2009 A(H1N1) influenza viruses and its transmissibility are not completely understood. The present study shows that overall morbidity and lung viral titers were higher in ferrets infected with 2009 A(H1N1) influenza virus isolates as compared with those infected with the seasonal H1N1 virus. Moreover, the detection of 2009 A(H1N1) influenza viruses in the intestinal tissue of ferrets is consistent with gastrointestinal involvement among some human 2009 A(H1N1) cases (*6*). Although the 2009 A(H1N1) influenza viruses demonstrated similar replication kinetics as the seasonal H1N1 virus in the upper respiratory tract of inoculated ferrets, the 2009 A(H1N1) influenza viruses did not spread to all naïve ferrets by means of respiratory droplets. This lack of efficient respiratory droplet transmission suggests that additional virus adaptation in mammals may be required to reach the high-transmissible phenotypes observed with seasonal H1N1 or the 1918 pandemic virus (*14*, *17*).

It was demonstrated previously (*17*) that the efficiency of respiratory droplet transmission in ferrets correlates with the α2-6–binding affinity of the viral HA. In fact, a single amino acid mutation in HA of the efficiently transmitting SC18 virus led to a virus (NY18) that transmitted inefficiently (fig. S5). The α2-6–binding affinity of NY18 HA was substantially lower than that of SC18 HA (fig. S5). In a similar fashion, the substantially lower α2-6–binding affinity of CA/04 HA than that of SC18 HA correlates with the less efficient 2009 A(H1N1) influenza virus respiratory droplet transmission (fig. S5).

Adaptation of the polymerase basic protein 2 (PB2) is also critical for efficient aerosolized respiratory transmission of an H1N1 influenza virus (*14*, *17*, *23*). A single amino acid substitution from glutamic acid to lysine at amino acid position 627 supports efficient influenza virus replication at the lower temperature (33°C) found in the mammalian airway and contributes to efficient transmission in mammals (*14*, *23*). All three of the 20th-century influenza pandemics were caused by viruses containing human adapted PB2 genes, and in general lysine is present at position 627 among the human influenza viruses, whereas a glutamic acid is found in this position among the avian influenza isolates that fail to transmit efficiently among ferrets (*14*). In contrast to the Brisbane/07 virus and other seasonal H1N1 viruses, all 2009 A(H1N1) influenza viruses to date with an avian influenza lineage PB2 gene possess a glutamic acid at residue 627 (*1*). The phenotype of PB2 is determined by the amino acid at position 627, which can arise by mutant selection or reassortment, and along with adaptive changes in the RBS should be closely monitored as markers for enhanced virus transmission.

References and Notes

1. R. J. Garten *et al.*, *Science* **325**, 5937 (2009); published online 22 May 2009 (10.1126/science.1176225).
2. *MMWR Morb. Mortal. Wkly. Rep.* **58**, 453 (2009).
3. *MMWR Morb. Mortal. Wkly. Rep.* **58**, 400 (2009).
4. *MMWR Morb. Mortal. Wkly. Rep.* **58**, 467 (2009).
5. http://www.who.int/en/
6. F. S. Dawood *et al.*, *J. Med.* **360**, 2605 (2009).
7. C. Fraser *et al.*, *Science* **324**, 1557 (2009); published online 11 May 2009 (10.1126/science.1176062).
8. T. M. Tumpey, J. A. Belser, *Annu. Rev. Microbiol.* **63**, 252 (2009).
9. R. J. Webby, R. G. Webster, *Science* **302**, 1519 (2003).
10. C. Viboud *et al.*, *Vaccine* **24**, 6701 (2006).
11. T. R. Maines *et al.*, *Proc. Natl. Acad. Sci. U.S.A.* **103**, 12121 (2006).
12. J. A. Belser *et al.*, *Proc. Natl. Acad. Sci. U.S.A.* **105**, 7558 (2008).
13. A. C. Lowen, P. Palese, *Infect. Disord. Drug Targets* **7**, 318 (2007).
14. N. Van Hoeven *et al.*, *Proc. Natl. Acad. Sci. U.S.A.* **106**, 3366 (2009).
15. Materials and methods are available as supporting material on *Science* Online.
16. H. L. Yen *et al.*, *J. Virol.* **81**, 6890 (2007).
17. T. M. Tumpey *et al.*, *Science* **315**, 655 (2007).
18. A. Srinivasan *et al.*, *Proc. Natl. Acad. Sci. U.S.A.* **105**, 2800 (2008).
19. A. Chandrasekaran *et al.*, *Nat. Biotechnol.* **26**, 107 (2008).
20. V. Soundararajan *et al.*, *Nat. Biotechnol.* **27**, 510 (2009).
21. C. A. Hartley, P. C. Reading, A. C. Ward, E. M. Anders, *Arch. Virol.* **142**, 75 (1997).
22. T. R. Maines *et al.*, *J. Virol.* **79**, 11788 (2005).
23. J. Steel, A. C. Lowen, S. Mubareka, P. Palese, *PLoS Pathog.* **5**, e1000252 (2009).

24. We thank P. Blair (Naval Health Research Center, San Diego), G. J. Demmler (Texas Children's Hospital, Houston), C. Alpuche-Aranda [Instituto de Diagnóstico y Referencia Epidemiológicos, Mexico], and the WHO Collaborating Centre for Reference and Research on Influenza (Melbourne) for facilitating access to viruses. We also thank X. Lu and A. Balish for preparation of viruses and V. Veguilla for statistical analysis. R.S. acknowledges the consortium for functional glycomics for providing glycan standards and support from the Singapore-MIT Alliance for Research and Technology and the National Institute of General Medical Sciences of the NIH (GM 57073 andU54 GM62116). Confocal microscopy of the human lung tissue sections was performed at the W. M. Keck Foundation Biological Imaging Facility at the Whitehead Institute. The findings and conclusions in this report are those of the authors and do not necessarily reflect the views of the funding agency.

Supporting Online Material

www.sciencemag.org/cgi/content/full/1177238/DC1
Materials and Methods
Figs. S1 to S5
Table S1
References

3 June 2009; accepted 23 June 2009
Published online 2 July 2009;
10.1126/science.1177238
Include this information when citing this paper.

Chlamydomonas Swims with Two "Gears" in a Eukaryotic Version of Run-and-Tumble Locomotion

Marco Polin,[1] Idan Tuval,[1] Knut Drescher,[1] J. P. Gollub,[1,2] Raymond E. Goldstein[1]*

The coordination of eukaryotic flagella is essential for many of the most basic processes of life (motility, sensing, and development), yet its emergence and regulation and its connection to locomotion are poorly understood. Previous studies show that the unicellular alga *Chlamydomonas*, widely regarded as an ideal system in which to study flagellar biology, swims forward by the synchronous action of its two flagella. Using high-speed imaging over long intervals, we found a richer behavior: A cell swimming in the dark stochastically switches between synchronous and asynchronous flagellar beating. Three-dimensional tracking shows that these regimes lead, respectively, to nearly straight swimming and to abrupt large reorientations, which yield a eukaryotic version of the "run-and-tumble" motion of peritrichously flagellated bacteria.

One of the most highly conserved structures among eukaryotes is the flagellum (*1*, *2*), whose composition in humans is nearly identical to that in unicellular algae (*3*). Because the coordinated motion of flagella is involved in fluid transport in the respiratory system (*4*), embryonic left-right asymmetry (*5*, *6*), intercellular communication (*7*), and possibly the evolution of multicellularity (*8*), it is important to understand the origin of flagellar synchronization. An emerging hypothesis (*9*–*12*) implicates hydrodynamic interactions, yet experimental proof is lacking. Flagellar synchronization is also important for prokaryotes, in which "run-and-tumble"

[1]Department of Applied Mathematics and Theoretical Physics, University of Cambridge, Wilberforce Road, Cambridge CB3 0WA, UK. [2]Department of Physics, Haverford College, Haverford, PA 19041, USA.

*To whom correspondence should be addressed. E-mail: R.E.Goldstein@damtp.cam.ac.uk

chemotaxis relies on the stochastic bundling and unbundling of flagella (*13*), resulting in individual random walks and the diffusion of populations (*14*).

Here, we ask whether eukaryotic locomotion has any relationship to the run-and-tumble paradigm, using the alga *Chlamydomonas reinhardtii* as a model (*15*, *16*). Its two flagella are termed cis and trans because of their positions relative to the eyespot, a rudimentary light-sensing organelle. Analysis of cells in the dark, over short (1- to 2-s) intervals (*17*, *18*), has shown two behaviors. Most cells (~95%) beat with a synchronous breaststroke interrupted occasionally by extra beats ("slips") of the trans flagellum, a phenomenon confirmed by later experiments over much longer periods (*19*). In this regime, cells swim in a tight helix along an almost straight center line. The remaining cells (~5%) beat asynchronously, with a large interflagellar frequency difference (10 to 30%), compatible with observations on demembranated cells (*20*), where trans flagella often beat with a higher frequency than cis flagella. These results have been interpreted as representative of distinct subpopulations. However, the underlying biochemical or physical processes that control synchronization remain unknown.

Previous studies tracking *C. reinhardtii* swimming (*21*–*23*) suggest that, like bacteria, entire populations display diffusive behavior. Existing interpretations (*22*) attribute diffusion to the accumulation of small deflections but lack explicit references to the actual beating dynamics of the flagella.

Here, we present three main experimental results on the beating of *C. reinhardtii* flagella and its relationship to swimming in the dark, where phototactic reorientations do not occur. First, we demonstrate that individual cells stochastically switch over the course of time between the two regimes: synchronous with slips and asynchronous. Second, we show that either the cis or the trans flagellum can be the faster one during asynchrony, so although their phototactic responses are intrinsically different (*17*, *18*, *20*), there is no absolute frequency asymmetry. Third, we present strong evidence that the diffusion of populations of *C. reinhardtii* is the result of localized events of large nonphototactic reorientations, corresponding to periods of asynchronous flagellar beating. Taken together, these results strongly suggest that the beating frequencies themselves are under the control of the cell. The stochastic movement back and forth between synchrony and asynchrony is reminiscent of the run-and-tumble motion of bacteria, with sharp turns taking the place of tumbles.

We first studied (*24*) the diffusion of a population of *C. reinhardtii* by gently centrifuging a dilute suspension of cells to the bottom of a plastic cuvette and analyzing the dynamics of the concentration profile as it spread upward (Fig. 1, A and B). In a region far from the bottom of the chamber, where cell-cell interactions are rare, the concentration flux is a linear function of the concentration gradient (Fig. 1C), and the slope of the fitted line gives then an estimate of the diffusion constant for an isolated individual: $D_{exp} = (0.68 \pm 0.11) \times 10^{-3}$ cm^2/s. A random walk of typical speed u and free-flight time τ gives a diffusion constant $D \sim u^2\tau$, implying a characteristic time on the order of 5 to 10 s for $u \sim 100$ μm/s.

To interpret this time and connect the macroscopic diffusive behavior to the dynamics of individual cells, we analyzed in a separate experiment high-speed movies of the flagella pairs of isolated *C. reinhardtii* cells held by micropipettes. The fact that a given cell moves back and forth between synchronous and asynchronous states is illustrated in Fig. 2. Figure 2A shows time series of the individual signals from the left and right flagella over a short (0.5-s) interval within a period of synchrony several seconds long, whereas Fig. 2B displays the asynchronous state in which the interflagellar phase difference drifts linearly in time

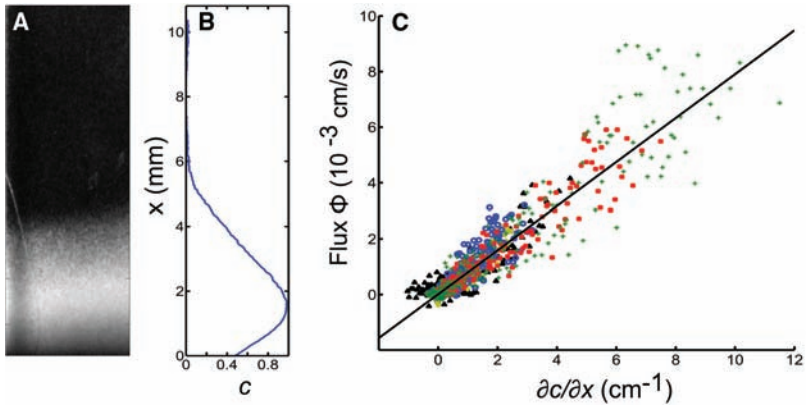

Fig. 1. Diffusive behavior of a population of *C. reinhardtii* containing thousands of individual cells. (**A**) Light scattered from the cells 1 min after being spun in a centrifuge. (**B**) Integrated light intensity as a function of height x. (**C**) Flux versus concentration gradient at various points in space and time; the linearity shows that cells spread according to Fick's law. Different-colored symbols correspond to independent trials.

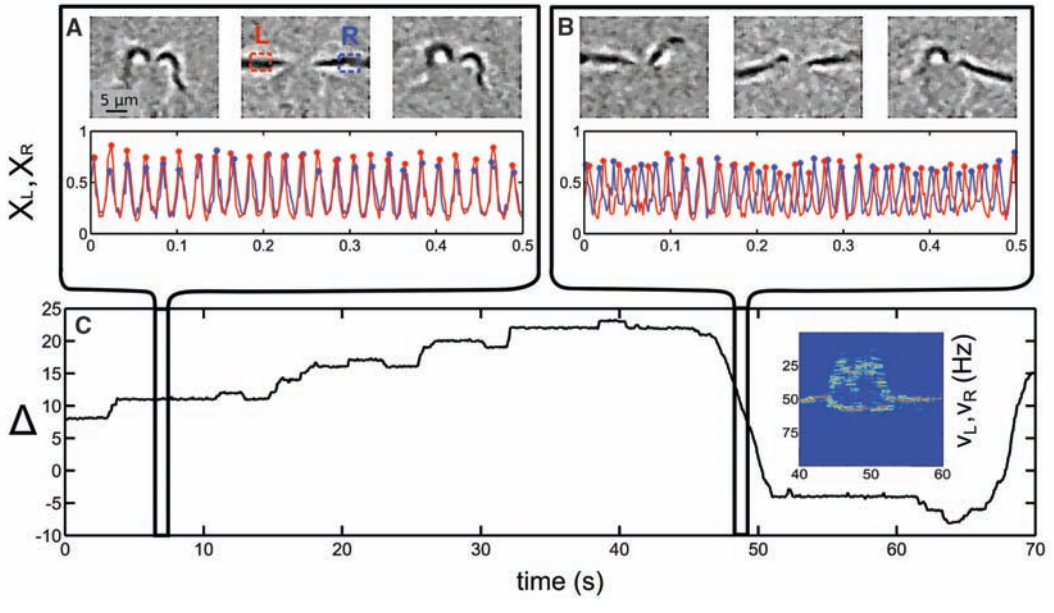

Fig. 2. A single *C. reinhardtii* cell moves back and forth between synchronous (**A**) and asynchronous (**B**) states. Movie frames showing a few cycles and the oscillatory intensity signals $X_{L,R}(t) = \Gamma_{L,R}(t)\sin[2\pi\theta_{L,R}(t)]$ (X, signal; L, left; R, right; Γ, amplitude; t, time; θ, phase), obtained by local sampling of the video light intensity near the two flagella, are shown for both cases. (**C**) A long (70-s) time series of the phase difference $\Delta(t) = \theta_L(t) - \theta_R(t)$ contains periods of synchrony interrupted by drifts of either sign. A windowed Fourier transform of the beating signals during the transition from synchronization to drifting and then back again to synchrony (inset) shows a large frequency difference in the asynchronous state. This behavior was characteristic of all 24 observed cells.

over tens of cycles. These short intervals are part of a much longer measurement window of 70 s (Fig. 2C). In this long time series, we see that drifts extend over periods of 1 to 3 s and can be of either sign. The interflagellar frequency difference during drifts is in the range from 10 to 30% of the mean (inset Fig. 2C). Synchronous intervals are more frequently interrupted by much shorter events (~0.2 s) resulting in a single extra beat of one flagellum: a phase slip. Slips can be of either sign, but are biased in one direction, constant throughout each experiment, and happen randomly in time. This behavior was characteristic of all the observed cells (*24*).

On a basic level, the two flagella of *C. reinhardtii* are oscillators, coupled through the fluid in which they move and possibly the cell wall through which they emerge, and subject to noise of both thermal and biochemical origin. Despite their complexity, the basic phenomenology can be captured by a simple mathematical model describing the dynamics of weakly coupled self-sustained noisy oscillators (*24*, *25*). Three parameters characterize this model: the interflagellar coupling strength ε, the flagellar noise intensity T_{eff}, and the intrinsic frequency difference between the two flagella $\delta\nu$, which can be determined even in the synchronized state and is responsible for the bias in the distribution of slips. The distribution of the measured coupling strengths ε (Fig. 3A) shows a well-defined peak at a value that compares very well with a rough estimate ε_m given by an idealized flagellar model with hydrodynamic coupling (*24*). This suggests that fluid flow is indeed the major contribution to the coupling responsible for flagellar synchronization.

Synchronous and asynchronous states cluster into two regions in parameter space, separated by nearly two orders of magnitude in the intrinsic interflagellar frequency difference (Fig. 3B), with no cells at intermediate values. These two distinct dynamical regimes are analogous to two distinct internal "gears." In the lower gear (a lower value of $\delta\nu$), the intrinsic interflagellar frequency difference is sufficiently small for the coupling to lead to robust synchronization. In the upper gear, the flagella beat with a high intrinsic frequency difference, and the coupling is too weak to cause significant frequency entrainment. Because individual cells alternate in time between these two regimes, we conclude that *C. reinhardtii* can control the state of synchronization of its flagella by actively changing their intrinsic frequency difference.

The stochastic switching between synchrony and asynchrony has clear effects on swimming trajectories. Figure 4A shows a portion of the

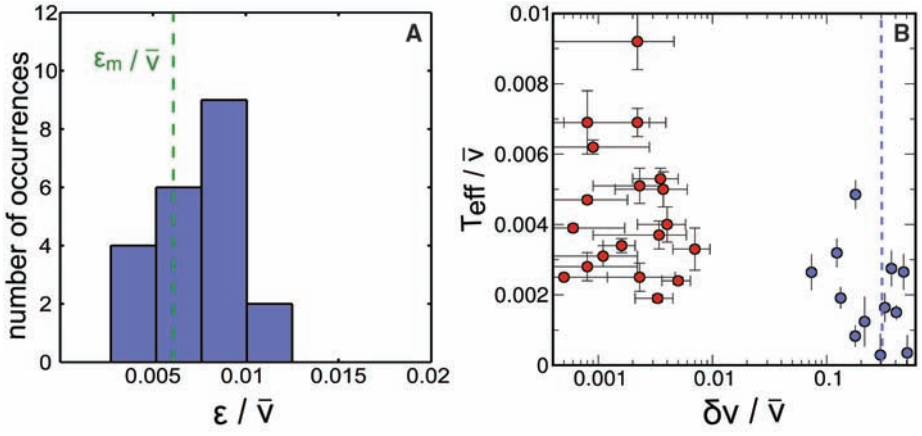

Fig. 3. Parameters of the phase synchronization model (*24*) extracted from high-speed imaging studies of flagellar dynamics, rescaled by the mean flagellar beating frequency $\bar{\upsilon}$. (**A**) The probability distribution of the coupling amplitude $\varepsilon/\bar{\upsilon}$ shows a well-defined peak at 0.0076, comparable to the estimate $\varepsilon_m/\bar{\upsilon}$ = 0.006 based on hydrodynamic interactions. (**B**) Data clustering in the parameter space defined by the intrinsic interflagellar frequency difference $\delta\nu$ and the flagellar noise intensity T_{eff} supports the existence of two distinct regimes. Although the noise differences are modest, the relative intrinsic frequency differences span two orders of magnitude, from 0.001–0.01 to 0.1–0.4. The dashed vertical line represents the intrinsic frequency difference observed in cell models (*20*).

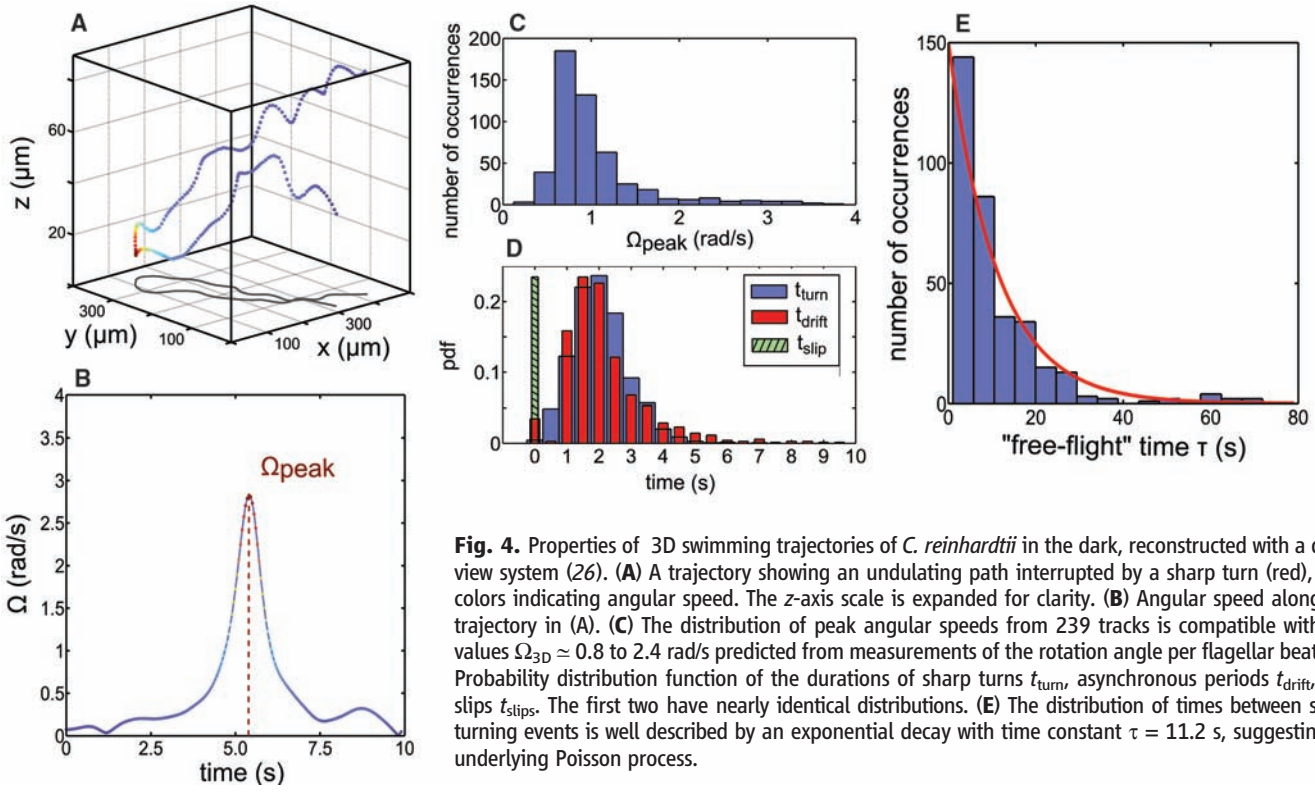

Fig. 4. Properties of 3D swimming trajectories of *C. reinhardtii* in the dark, reconstructed with a dual-view system (*26*). (**A**) A trajectory showing an undulating path interrupted by a sharp turn (red), with colors indicating angular speed. The *z*-axis scale is expanded for clarity. (**B**) Angular speed along the trajectory in (A). (**C**) The distribution of peak angular speeds from 239 tracks is compatible with the values $\Omega_{3D} \simeq 0.8$ to 2.4 rad/s predicted from measurements of the rotation angle per flagellar beat. (**D**) Probability distribution function of the durations of sharp turns t_{turn}, asynchronous periods t_{drift}, and slips t_{slips}. The first two have nearly identical distributions. (**E**) The distribution of times between sharp turning events is well described by an exponential decay with time constant τ = 11.2 s, suggesting an underlying Poisson process.

three-dimensional (3D) reconstruction (*26*) of a trajectory containing both helical swimming and a clearly recognizable sharp turning event (Fig. 4B). Analysis of hundreds of sharp turns from 3D trajectories (*24*) yields the probability distribution of their angular speeds (Fig. 4C) and duration (Fig. 4D). The range of angular speeds is consistent with an estimate derived from the average frequency difference during asynchronous beating periods and the average angular rotation of the cell body per flagellar beat (*24*). The distribution of durations of turns is nearly identical to that of drifts (Fig. 4D) and incompatible with that of slips, the only other observed behavior that could lead to turns in the dark. These results indicate that sharp turns are the direct consequence of periods of asynchronous flagellar beating. Because sharp turns are defined by angular speeds much higher than typical background rates (Fig. 4B), we choose to consider these as the only turning events, which separate straight-line free-flight segments. The probability distribution of the duration of such free flights, shown in Fig. 4E, decays exponentially with a mean of $\tau = 11.2$ s. This time scale is clearly the one inferred earlier from the macroscopic diffusion measurements. The diffusion constant D can be estimated more precisely with the well-known results from run-and-tumble random walk models (*14*). With the average parameters extracted from the 3D trajectories, we obtain (*24*) $D \cong (0.47 \pm 0.05) \times 10^{-3}$ cm^2/s, which is in very good agreement with the value estimated from the macroscopic measurements on large populations.

We have found that in the dark, *C. reinhardtii* can vary the intrinsic frequencies of its two flagella so that they alternate between synchronous and asynchronous beating, with synchrony realized though a mechanism consistent with hydrodynamic coupling. This leads to swimming trajectories with stochastically distributed sharp turns and ultimately to the diffusive behavior of a population. In contrast to previous observations on cell models (*20*), we showed that in each cell either flagellum can beat faster than the other. This approximate symmetry is a strong indication that the unknown regulatory system at work here is distinct from that governing phototaxis, which is based instead on opposite amplitude modulations of flagellar motion, and it shows that the idea of a well-defined intrinsic frequency difference between cis and trans flagella is incorrect. Such control mechanisms could also have a role in coordinating large numbers of cilia in simple multicellular organisms lacking a central nervous system (such as *Volvox*). Open issues include the origins of this regulation, the characteristic time scale between asynchronous intervals, and the noise of flagellar beats, along with the possible interplay of these processes with chemotaxis and phototaxis.

References and Notes

1. I. Ibañez-Tallon, N. Heintz, H. Omran, *Hum. Mol. Genet.* **12**, R27 (2003).
2. G. J. Pazour, N. Agrin, J. Leszyk, G. B. Witman, *J. Cell Biol.* **170**, 103 (2005).
3. D. R. Mitchell, *J. Phycol.* **36**, 261 (2000).
4. B. A. Afzelius, *Science* **193**, 317 (1976).
5. S. Nonaka *et al.*, *Cell* **95**, 829 (1998).
6. J. H. E. Cartwright, O. Piro, I. Tuval, *Proc. Natl. Acad. Sci. U.S.A.* **101**, 7234 (2004).
7. Q. Wang, J. Pan, W. J. Snell, *Cell* **125**, 549 (2006).
8. C. A. Solari, S. Ganguly, J. O. Kessler, R. E. Michod, R. E. Goldstein, *Proc. Natl. Acad. Sci. U.S.A.* **103**, 1353 (2006).
9. S. Gueron, K. Levit-Gurevich, *Proc. Natl. Acad. Sci. U.S.A.* **96**, 12240 (1999).
10. B. Guirao, J. F. Joanny, *Biophys. J.* **92**, 1900 (2007).
11. A. Vilfan, F. Julicher, *Phys. Rev. Lett.* **96**, 058102 (2006).
12. T. Niedermayer, B. Eckhardt, P. Lenz, *Chaos* **18**, 037128 (2008).
13. H. C. Berg, D. A. Brown, *Nature* **239**, 500 (1972).
14. H. C. Berg, *Random Walks in Biology* (Princeton Univ. Press, Princeton, NJ, 1983).
15. C. Ainsworth, *Nature* **448**, 638 (2007).
16. *The Chlamydomonas Sourcebook*, E. H. Harris, D. Stern, G. Witman, Eds. (Elsevier, Oxford, ed. 2, 2009).
17. U. Rüffer, W. Nultsch, *Cell Motil.* **7**, 87 (1987).
18. U. Rüffer, W. Nultsch, *Cell Motil.* **41**, 297 (1998).
19. K. Josef, J. Saranak, K. W. Foster, *Cell Motil. Cytoskeleton* **61**, 83 (2005).
20. N. Okita, N. Isogai, M. Hirono, R. Kamiya, K. Yoshimura, *J. Cell Sci.* **118**, 529 (2005).
21. V. A. Vladimirov, M. S. C. Wu, T. J. Pedley, P. V. Denissenko, S. G. Zakhidova, *J. Exp. Biol.* **207**, 1203 (2004).
22. N. A. Hill, D.-P. Häder, *J. Theor. Biol.* **186**, 503 (1997).
23. P. Hegemann, B. Bruck, *Cell Motil.* **14**, 501 (1989).
24. Materials and methods are available as supporting material on *Science* Online.
25. A. Pikovsky, M. Rosenblum, J. Kurths, *Synchronization. A Universal Concept in Nonlinear Science* (Cambridge Univ. Press, Cambridge, 2001).
26. K. Drescher, K. Leptos, R. E. Goldstein, *Rev. Sci. Instrum.* **80**, 014301 (2009).

27. We thank K. Leptos, T. J. Pedley, C. A. Solari, K. Visscher, A. Nedelcu, D. Page-Croft, T. Parkin, and N. Price and acknowledge support from the Marie-Curie Program (M.P.), the Human Frontiers Science Program (I.T.), the Leverhulme Trust (J.P.G.), the Biotechnology and Biological Sciences Research Council, the Engineering and Physical Sciences Research Council, the U.S. Department of Energy, and the Schlumberger Chair Fund.

Supporting Online Material

www.sciencemag.org/cgi/content/full/325/5939/487/DC1
Materials and Methods
Figs. S1 to S3
References

23 February 2009; accepted 2 June 2009
10.1126/science.1172667

Translocator Protein (18 kD) as Target for Anxiolytics Without Benzodiazepine-Like Side Effects

Rainer Rupprecht,[1,2]* Gerhard Rammes,[2,3] Daniela Eser,[1] Thomas C. Baghai,[1] Cornelius Schüle,[1] Caroline Nothdurfter,[1,2] Thomas Troxler,[4] Conrad Gentsch,[4] Hans O. Kalkman,[4] Frederique Chaperon,[4] Veska Uzunov,[4] Kevin H. McAllister,[4] Valerie Bertaina-Anglade,[5] Christophe Drieu La Rochelle,[5] Dietrich Tuerck,[6] Annette Floesser,[4] Beate Kiese,[7] Michael Schumacher,[8] Rainer Landgraf,[2] Florian Holsboer,[2] Klaus Kucher[4]

Most antianxiety drugs (anxiolytics) work by modulating neurotransmitters in the brain. Benzodiazepines are fast and effective anxiolytic drugs; however, their long-term use is limited by the development of tolerance and withdrawal symptoms. Ligands of the translocator protein [18 kilodaltons (kD)] may promote the synthesis of endogenous neurosteroids, which also exert anxiolytic effects in animal models. Here, we found that the translocator protein (18 kD) ligand XBD173 enhanced γ-aminobutyric acid–mediated neurotransmission and counteracted induced panic attacks in rodents in the absence of sedation and tolerance development. XBD173 also exerted antipanic activity in humans and, in contrast to benzodiazepines, did not cause sedation or withdrawal symptoms. Thus, translocator protein (18 kD) ligands are promising candidates for fast-acting anxiolytic drugs with less severe side effects than benzodiazepines.

Anxiety disorders are highly prevalent disabling disorders (*1*) that frequently turn into chronic clinical conditions (*2*). Benzodiazepines such as diazepam are fast-acting and effective antianxiety agents (*3*–*5*) and the most commonly prescribed anxiolytics. However, their side effects such as sedation and, following chronic administration, development of tolerance, consecutive abuse liability, and withdrawal symptoms render their use problematic in the long-term treatment of anxiety disorders (*2*–*4*). Currently, antidepressants such as selective serotonin reuptake inhibitors are first-line treatment for most anxiety disorders. However, their anxiolytic effects occur only after several weeks of treatment (*2*–*4*). Thus, there is need for anxiolytic agents that retain the rapid anxiolytic potential of benzodiazepines but lack their unfavorable side effects.

Neurosteroids are synthesized from cholesterol or steroidal precursors and modulate neurotransmitter receptors (*6*–*8*). Ring A–reduced neurosteroids are endogenous metabolites of the hormone progesterone and potent positive allosteric modulators of γ-aminobutyric acid type A ($GABA_A$) receptors, which mediate the effects of the inhibitory neurotransmitter GABA in the mammalian nervous system (*6*–*8*). They exert pronounced anxiolytic effects in animal models (*9*–*11*), and their concentrations are reduced